Journal of Mechanics in Medicine and Biology

ROLE OF OXYGEN CONCENTRATION IN THE OSTEOBLASTS BEHAVIOR: A FINITE ELEMENT MODEL

PAU URDEITX[1,2,3], SOLMAZ FARZANEH[4], S. JAMALEDDIN MOUSAVI[4] and MOHAMED H. DOWEIDAR*[1,2,3]

[1]*Mechanical Engineering Department*
School of Engineering and Architecture (EINA)
University of Zaragoza
Zaragoza, Spain

[2]*Aragón Institute of Engineering Research (I3A)*
University of Zaragoza
Zaragoza, Spain

[3]*Biomedical Research Networking Center in Bioengineering*
Biomaterials and Nanomedicine (CIBER-BBN)
Zaragoza, Spain
**mohamed@unizar.es*

[4]*Mines Saint-Etienne, Univ Lyon, Univ Jean Monnet, INSERM, U 1059, Sainbiose, Centre CIS, F - 42023, Saint-Etienne, France*

Oxygen concentration plays a key role in cell survival and viability. Besides, it has important effects on essential cellular biological processes such as cell migration, differentiation, proliferation and apoptosis. Therefore, the prediction of the cellular response to the alterations of the oxygen concentration can help significantly in the advances of cell culture research. Here, we present a 3D computational mechanotactic model to simulate all the previously mentioned cell processes under different oxygen concentrations. With this model, three cases have been studied. Starting with mesenchymal stem cells within an extracellular matrix with mechanical properties suitable for its differentiation into osteoblasts, and under different oxygen conditions to evaluate their behavior under normoxia, hypoxia and anoxia. The obtained results, which are consistent with the experimental observations, indicate that cells tend to migrate toward zones with higher oxygen concentration where they accelerate their differentiation and proliferation. This technique can be employed to control cell migration toward fracture zones to accelerate the healing process. Besides, as expected, to avoid cell apoptosis under conditions of anoxia and to avoid the inhibition of the differentiation and proliferation processes under conditions of hypoxia, the state of normoxia should be maintained throughout the entire cell-culture process.

Keywords: Finite element modeling; osteoblasts; mesenchymal stem cells; cell migration; differentiation; proliferation; apoptosis; anoxia; hypoxia; normoxia.

*Corresponding author.

1. Introduction

The processes of tissue regeneration and remodeling significantly depend on the mechanisms of cell migration, differentiation, proliferation and apoptosis. These mechanisms are regulated by a complex combination of mechanical,[1–4] chemical,[5–8] thermal[9] and electrical[10,11] cues. For instance, during wound healing, a cascade of electrical, chemical and mechanical cues is produced.[12–14] In the first stages of wound healing, those signals induce migration of certain cell types, such as fibro-blasts and endothelial cells, toward the wound zone. Sequentially, those cues guide the cells to promote the creation of new extracellular matrix (ECM), new blood vessels and to repopulate the wound with the appropriate cells, restoring the damaged tissue.

In general, cells have the ability to interact with their environment through mechanotaxis and chemotaxis, allowing them to recognize the stiffness and the topography of the environment as well as the presence of nutrients and different proteins. In the last two decades, great effort has been devoted to understand how the cell environment affects its decision of migration, differentiation, and proliferation.[1,2,15–17] Some of these studies have made it possible to guide cell differentiation through mechanical and chemical stimulation to a certain cell type. The use of these techniques, in conjunction with autologous induced pluripotent stem cells (iPSC), has opened a new range of possibilities in the treatment of many diseases. However, only a little knowledge of the regeneration process has been acquired and many cell behaviors are still unstudied. Thus, knowing and controlling the stimuli that govern cell behavior is the first step to improve the tissue regeneration process.

One of the major factors, and probably the most important, for tissue regeneration, is the lack of oxygen (hypoxia). During cell culture, the cell can experience a wide range of oxygen concentrations, which directly affect its viability. Cells that have a normal oxygen concentration (normoxia) can demonstrate normal activities such as migration, differentiation and proliferation.[4,16–18] Depending on the cell type, there are different thresholds of oxygen concentration for the normoxia state. For instance, cartilage, which is an avascular tissue, has typical concentrations of 1–6%[14] while this range of oxygen concentration changes in the case of the bone to 6–13%[19] When this level falls, it causes a deficit between the available oxygen and that is necessary to maintain the activity of the cells. Under these conditions, it is considered that the cell is under hypoxic condition.[14,20] Under hypoxic conditions, cell viability,[21] prolifer-ation,[22] differentiation,[14] and cell migration[22] may get affected. Although a worse situation is expected for the cells under hypoxia, some experiments have shown an enhancement in cell proliferation under certain hypoxic thresholds.[7,21,22] For in-stance, under hypoxia, osteoblasts show a reduction in cell prolifera-tion,[23] whereas in fibroblasts there is an increase in cell proliferation.[24] In contrast, in both cases, an increase in cell apoptosis is also observed. These contradictory processes provide improved capacity for the cells to remodel their tissue. In the most

dramatic case, when there is an almost total lack of oxygen, it is considered that the cell is under conditions of anoxia.[20,23] In such a case, cells will trigger apoptosis.

Oxygen concentration in the ECM plays a key role in bone regeneration. At the first phase of bone remodeling, an oxygen gradient with a high shortage of oxygen concentration in the center of the fracture healing is generated. Bosgraaf *et al.*[25] and Neilson *et al.*[26] have demonstrated that the effect of a chemical gradient is able to induce and guide cell migration. However, it has been observed that the effect of hypoxia not only induces migration, but also affects the gene expression of cells. Steinbrech *et al.*[23] and Warren *et al.*[27] found that under hypoxic conditions osteoblasts, fibroblasts and endothelial cells express Transforming Growth Factors (TGFs) and Vascular Endothelial Growth Factors (VEGFs), which promote angiogenesis process. More recently, Wan *et al.*[13] mentioned an improvement in the regeneration speed of bone tissues inducing hypoxia in osteoblasts.

In order to enhance the understanding of the roles of different cues in the process of tissue regeneration, many computational models, with different approaches, have been developed.[28–31] All these models are able to predict the general response of the cells to different received signals from their environment through the mechano, chemo, electro and thermotaxis. However, although many experimental studies infer the importance of the oxygen levels in tissue regeneration,[12–14,23,27] to the best of our knowledge, there are no models that consider the effects of oxygen concentration on cell migration, differentiation, proliferation and apoptosis. Therefore, the aim of this work is to develop a new numerical model to study the influence of oxygen concentration on cell migration, differentiation, proliferation and apoptosis.

2. Model Formulation

Recently, many advanced computational methods are developed to enhance the accuracy of the standard finite element method (FEM).[32,33] These methods are established to improve the precision and stability of traditional methods. In contrast, they may increase the computational cost. As the proposed model does not have any convergence or stability problems and the objective is to get the results at a reasonable calculation time, the standard FEM is employed to consider cell migration, differentiation, proliferation and apoptosis of mesenchymal stem cells (MSCs) and osteoblasts. The model enables us to define different chemical and mechanical conditions in the ECM to evaluate the cell response.[30,34–39]

2.1. *Cell migration*

Cell migration is conditioned by the capability of the cell to interact with its microenvironment.[40,41] The mechanical forces generated by the cell are a function of its internal stress, which is classified into active and passive stresses. Active stress, generated by the contraction of the actin and myosin II filaments, depends on a threshold of a maximum, $\varepsilon_{\max}$, and a minimum, $\varepsilon_{\min}$, internal strains of the cell.

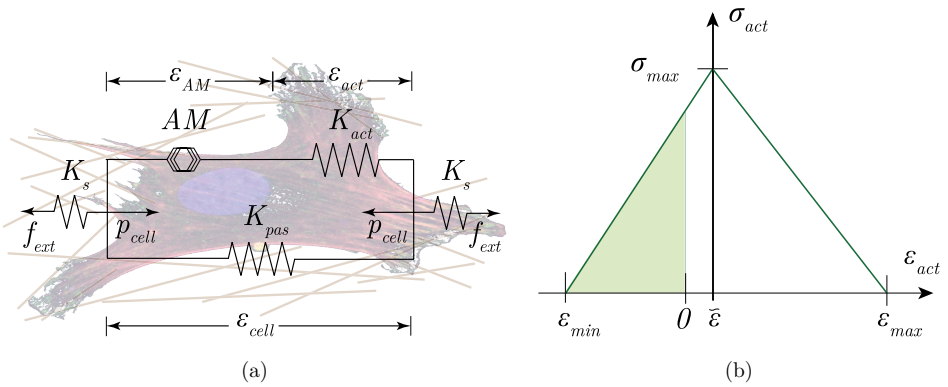

Fig. 1. Mechanosensing model. (a) The mechanical model of the actin–myosin machinery. K_{pas} is the stiffness of the passive elements of the cell, K_{act} is the stiffness of actin–myosin filaments and K_{s} is the ECM stiffness. f_{ext} and p_{cell} are the external forces over the cell and the internal stress of the cell, respectively. (b) The stress exerted by the actin–myosin machinery, σ_{act}, depends on the contractile strain of the cell, ε_{act}. $\varepsilon_{\min}$ and $\varepsilon_{\max}$ are the minimum and maximum deformation of the actin–myosin filaments.

Passive stress, related to the strain of passive elements such as the cell membrane and the cell cytoskeleton (CSK), is directly proportional to the strain and stiffness of the cell's passive elements. To sense the mechanical properties of its ECM, the cell exerts some sensing forces, which stress the ECM. The resultant stress, in turn, generates ECM strain. Therefore, the total stress transmitted to the ECM by the ith
node of the cell-ECM interface, which is the summation of the active and the passive stresses is given by

$$\boldsymbol{\sigma}_i = \begin{cases} K_{\text{pas}}\varepsilon_i, & \varepsilon_i < \varepsilon_{\min} \quad \text{or} \quad \varepsilon_i > \varepsilon_{\max}, \\ \dfrac{K_{\text{act}}\sigma_{\max}(\varepsilon_{\min} - \varepsilon_i)}{K_{\text{act}}\varepsilon_{\min} - \sigma_{\max}} + K_{\text{pas}}\varepsilon_i, & \varepsilon_{\min} \le \varepsilon_i \le \tilde{\varepsilon}, \\ \dfrac{K_{\text{act}}\sigma_{\max}(\varepsilon_{\max} - \varepsilon_i)}{K_{\text{act}}\varepsilon_{\max} - \sigma_{\max}} + K_{\text{pas}}\varepsilon_i, & \tilde{\varepsilon} \le \varepsilon_i \le \varepsilon_{\max}, \end{cases} \tag{1}$$

where K_{pas} and K_{act} are the stiffness of passive and active elements, respectively, ε_i is the cell internal strain at the ith node of the cell surface and $\sigma_{\max}$ is the maximum stress generated by the actin–myosin filaments, and $\tilde{\varepsilon}$ being defined by

$$\tilde{\varepsilon} = \sigma_{\max}/K_{\text{act}}. \tag{2}$$

For simplicity, during migration, a constant spherical morphology of the cell has been considered. For the calculation of the internal cell strain, we should define the deformation in each node of the cell surface located in the cell-ECM interface due to mechanosensing process. The sensing forces, which are exerted in each node of the cell surface toward the cell centroid (Fig. 2(a)), allow the cell to probe its environment. Hence, the strain in each node of the cell surface due to mechanosensing

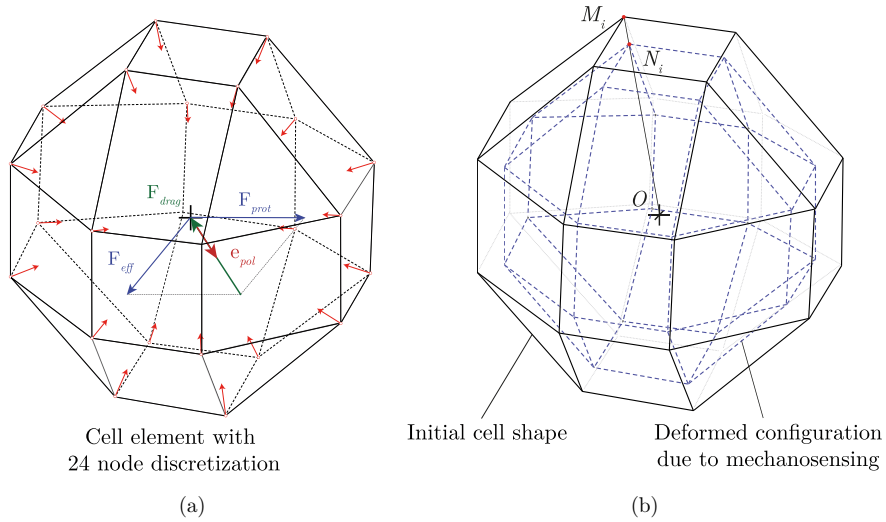

Fig. 2. Schematic configuration of the cell. (a) Mechanosensing process in which the sensing forces are exerted at each node of the cell surface toward the cell centroid. $\mathbf{F}_{\text{eff}}$, $\mathbf{F}_{\text{prot}}$, $\mathbf{F}_{\text{drag}}$ and $\mathbf{e}_{\text{pol}}$ are the effective force, the protrusion force, the drag force and a unit vector in the direction of the movement, respectively. (b) The cell is deformed due to mechanosensing process. The cell initial and deformed configuration are shown in the solid and dashed lines, respectively. Therefore, the nodal traction forces can be calculated based on the deformation of each node using Eq. (9).

process can be calculated as (see Fig. 2(b))

$$\varepsilon_i = \frac{M_i N_i}{OM_i}, \quad i = 1 : n, \tag{3}$$

where ε_i, M_iN_i and OM_i, represent the strain of the ith node on the cell surface, the displacement of the ith node in the sensing force direction due to mechanosensing process and the initial distance between the ith node and cell centroid, respectively. n is the number of nodes at the cell's surface (Fig. 2(b)). The variation of the de-formation among the nodes of the cell surface will contribute in the decision of the cell to migrate toward a determined direction based on the mechanosensing process. Here, we consider that the cell migrates toward the direction of the minimum internal deformation.

Three main forces, from three different sources, have been considered in this model to define the migration process. Therefore, assuming that the contribution of the cell inertia is negligible compared with the other forces due to the microscale problem, the force equilibrium reads

$$\mathbf{F}_{\text{eff}} + \mathbf{F}_{\text{prot}} + \mathbf{F}_{\text{drag}} = 0, \tag{4}$$

where $\mathbf{F}_{\text{eff}}$, $\mathbf{F}_{\text{prot}}$ and $\mathbf{F}_{\text{drag}}$ are the effective traction force, protrusion force and drag force, respectively. $\mathbf{F}_{\text{eff}}$ includes the contribution of the oxygen concentration and the mechanical effects on the cell traction force generated by the cell's internal

strains as shown in Eq. (5). The presence of an oxygen gradient in the ECM induces the polymerization of the actin–myosin fibrils guiding the direction of the pseudopods toward the higher oxygen concentration. This results in a direct effect on the polarization direction of the cell that tends to migrate toward zones of higher oxygen concentration.[42] Therefore, it can be considered that the variation of the oxygen concentration modifies the migration direction without modifying the force module as

$$\mathbf{F}_{\text{eff}} = \|\mathbf{F}^{\text{net}}_{\text{trac}}\|(\mu_{\text{mech}}\mathbf{e}_{\text{mech}} + \mu_{o_2}\mathbf{e}_{o_2}), \tag{5}$$

where μ_{mech} and μ_{o_2} represent the effectiveness of each signal with respect to the other. To keep the magnitude of $\mathbf{F}_{\text{eff}}$ of the same order of the traction force, the variables μ_{mech}, and μ_{o_2} should be defined such that $\mu_{\text{mech}} + \mu_{o_2} = 1$. Therefore, if one of them is more intensive than the other, it will have a higher effect on the effective force. Moreover, $\mathbf{e}_{\text{mech}}$ and $\mathbf{e}_{o_2}$ are unit vectors in the direction of oxygen and mechanical gradients. In the case of oxygen gradient, the unit vector can be defined through its respective gradient as

$$\mathbf{e}_{o_2} = \frac{\nabla[o_2]}{\|\nabla[o_2]\|}, \tag{6}$$

where ∇ is the gradient operator and $[o_2]$ is the oxygen concentration.

The unit vector corresponding to the mechanotaxis can be calculated by the sum of the traction forces applied at all the nodes of the cell located in the cell-ECM interface. Nodes with less deformation, in module, will experience a greater traction force. However, due to the direction of the exerted nodal traction forces (see Fig. 2(a)), the direction of mechanotaxis polarization (direction of the lowest cellular deformation) will correspond with the opposite direction to the resultant traction forces, $\mathbf{F}^{\text{net}}_{\text{trac}}$, as

$$\mathbf{e}_{\text{mech}} = -\frac{\mathbf{F}^{\text{net}}_{\text{trac}}}{\|\mathbf{F}^{\text{net}}_{\text{trac}}\|}. \tag{7}$$

The resultant traction force, $\mathbf{F}^{\text{net}}_{\text{trac}}$, is calculated by the summation of the traction forces applied at each node as

$$\mathbf{F}^{\text{net}}_{\text{trac}} = \sum_{i=1}^{n} \mathbf{F}^{\text{trac}}_{i}, \tag{8}$$

where n is the number of nodes located on the cell surface and $\mathbf{F}^{\text{trac}}_{i}$ is the nodal traction force, which is proportional to the cell internal stress, σ_i, obtained by Eq. (1). This force is the contribution of the internal actin–myosin machinery of the cell. It is transmitted to the ECM through the cell adhesions of the integrin family.[43,44] As long as we have discretized the cell body by finite elements, we have to define traction forces at each node of the cell surface. These forces are directly proportional to the cell surface, S and internal stress of the cell at each node of the cell surface,

σ_i, given by

$$\mathbf{F}_i^{\text{trac}} = \sigma_i S \zeta \mathbf{e}_i, \tag{9}$$

where $\mathbf{e}_i$ is a unit vector passing from the ith node located on the cell surface toward the cell centroid, and ζ is a dimensionless parameter that represents the adhesiveness of the cell , which can be calculated by

$$\zeta = k n_r \psi, \tag{10}$$

whereψ is a constant representing the concentration of ligands, k is a binding constant and n_r is the resultant of the number of available receptors at the front n_f and back n_b of the cell.

The protrusion force $\mathbf{F}_{\text{prot}}$ is a random force generated by the polymerization of actin filaments inside the cell.[41,45] This random polymerization generates extensions of the cell membrane through which the cell is able to create new binding points to the ECM that induce movement in that direction. Both the direction and the modulus of this force are defined randomly, but its modulus is always less than cell traction force Eq. (11).[29]

$$\mathbf{F}_{\text{prot}} = \kappa \|\mathbf{F}_{\text{net}}^{\text{trac}}\| \mathbf{e}_{\text{rand}}, \tag{11}$$

where κ is a randomly generated number between $0 \leq \kappa < 1$, and $\mathbf{e}_{\text{rand}}$ is a random unit vector that defines the direction of the protrusion force.

The drag force $\mathbf{F}_{\text{drag}}$ is an opposing resistance force to the cell movement due to the viscosity of the medium in which the cell migrates. This force is directly proportional to the cell velocity and it depends on the viscoelastic properties of the ECM.[29,34,46] In Stokes' regime, the drag force can be simplified as the drag force on a sphere of radius r moving at a velocity v in an ECM with a viscosity η.[29]

$$\|\mathbf{F}_{\text{drag}}\| = 6\pi r \eta v. \tag{12}$$

As the drag force, which is calculated by Eq. (4), opposes the cell movement, we can define the polarization direction of the cell (direction of the migration) by

$$\mathbf{e}_{\text{pol}} = -\frac{\mathbf{F}_{\text{drag}}}{\|\mathbf{F}_{\text{drag}}\|}. \tag{13}$$

Likewise, the cell velocity modulus, through Eq. (12), is given by

$$v = \frac{\|\mathbf{F}_{\text{drag}}\|}{6\pi r \eta}. \tag{14}$$

Therefore, the cell translocation at each time t can be calculated from the cell speed obtained in Eq. (14) by

$$d = vt\mathbf{e}_{\text{pol}}. \tag{15}$$

2.2. *Cell interaction*

When two or more cells are interacting simultaneously with the ECM, we should calculate strains, forces and velocity for each one as we have shown for one cell previously. If some cells are close enough to each other, the strains in the ECM caused by the activity of a cell will influence the calculation of the other one. In this way, the cells have the ability to feel each other through the mechanosensing mechanism.

During the migration process, we have to ensure that the limits between the cells are maintained in such a way that the interference of the cells with each other is prevented. As a constant spherical morphology of the cell is considered, we can simply calculate the distance between two cells as

$$\mathbf{x}_{ij} = \mathbf{x}_j - \mathbf{x}_i, \tag{16}$$

where $\mathbf{x}_i$ and $\mathbf{x}_j$ correspond to the position vector of the centroid of the ith and jth cells, respectively. It must always be fulfilled that $\|\mathbf{x}_{ij}\| \leq 2r$ for any pair of cells to prevent their interference (see Fig. 3).

When two cells are in contact, their cell membranes adapt to each other maintaining tangential contact between them in such a way that they are not able to extend pseudopods in the inter-contact area to interact with the ECM.[53,54]

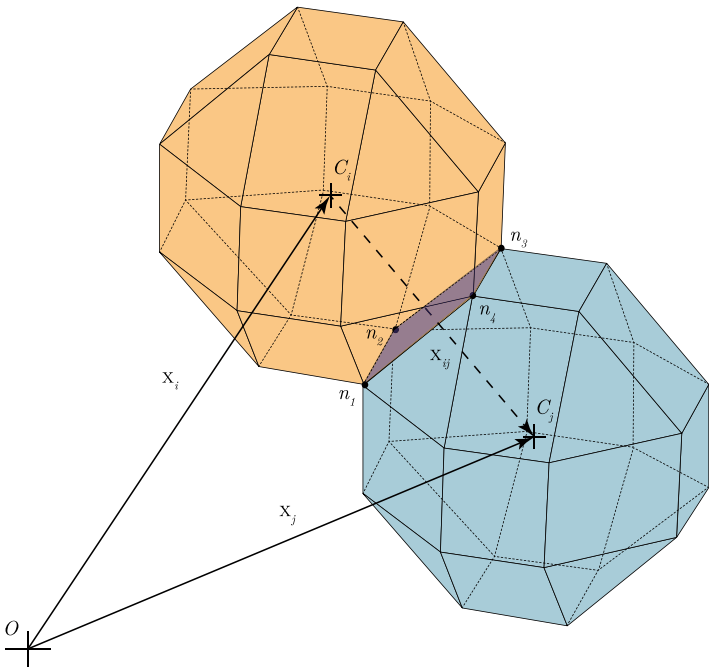

Fig. 3. Cell interaction. The $\mathbf{x}_i$ and $\mathbf{x}_j$ vectors are the centroid position vectors of the ith and jth cells, and $\mathbf{x}_{ij} \geq 2r$ is the distance between two cell centroids. The common nodes (such as $n_1 : n_4$) lose the ability to experiment the ECM.

Therefore, it has been considered that the in-contact nodes do not exert sensing forces to sense their ECM. It is worth to note that although there is no sensing force on these nodes, the cells will send out traction forces in these nodes as well.[36]

2.3. *Cell differentiation, proliferation and apoptosis*

The cell, through its interaction with the ECM, is able to recognize the conditions of its environment. In the current model, the equations that relate this process to the mechanical and chemical stimuli, described in the previous section, have been employed. These conditions have the potential to alter the cellular gene expression, guiding cell differentiation, proliferation and death processes. In this section, the processes of proliferation, differentiation and apoptosis are integrated into the previous model.

Since the discovery of stem cells, many works have been developed to understand what triggers the differentiation of these cells in different phenotypes. Nowadays, it is known that cell differentiation is promoted, among other stimuli, by a combination of mechanical and chemical factors that are present in the ECM. Engler *et al.*[4] studied the effects of matrix stiffness on the differentiation of the MSCs. They observed that the cells showed neurogenic markers in ECMs with stiffness similar to that of soft tissues (0.1–1 KPa), in ECMs of intermediate stiffness (8–15 KPa) appeared myogenic markers, and in stiff ECMs, similar to bone tissues (25–40 KPa), the cells had osteogenic markers. In ECMs with high stiffness, during the mechanosensing process, the cell undergoes a lower internal deformation, while in softer ECMs, the cell undergoes a higher internal deformation. These generated internal cell deformations are able to drive the cell destination.

Thus, in the current model, differentiation has been considered as a cellular response to the mechanical stimulus, which is related to the level of internal deformation of the cell. From the equations described in the previous section, it is possible to obtain the mechanical deformation of each node, γ_i, projecting the corresponding nodal deformation tensor of $\boldsymbol{\epsilon}_i$ in the polarization direction of the cell (Eq. (13))

$$\boldsymbol{\gamma}_i = \mathbf{e}_{\text{pol}} : \boldsymbol{\epsilon}_i : \mathbf{e}_{\text{pol}}^T. \tag{17}$$

It is worth noting that cell differentiation is not an instantaneous process, but it depends on the received signal during cell maturation that regulates cell fate.[55,56] Thereby, we consider the mechanical signal as a time-dependent signal during the cycle of cell maturation. Thus, the cell internal deformation in the cell polarization direction can be defined at time t by

$$\boldsymbol{\gamma}(\mathbf{x}, t) = \sum_{i=1}^{n} \boldsymbol{\gamma}_i, \tag{18}$$

where $\gamma(\mathbf{x}, t)$ represents the level of the cell mechanical signal at time t.

The maturation cycle reflects the time that the cell needs to recognize and adapt itself to the new environment in such a way to be able to differentiate into the

proper cell type. This cycle establishes the minimum time from which changes in the cell gene expression can be observed, and is partially dependent on the level of mechanical stimulation experienced by the cell.[31] Wu *et al.*[57] studied the differentiation of chondrocytes under different loading states. They observed that the time needed for cell differentiation varied for cells cultured under different loading conditions. In this model, a linear relationship has been assumed between the maturation time and the mechanical stimulus. Therefore, the maturation time of each cell will be defined by

$$t_{\text{mat}}(\gamma, t) = t_{\text{min}} + t_p \gamma(\mathbf{x}, t), \tag{19}$$

where $t_{\text{mat}}(\gamma, t)$ is the time required by the cell to maturate, t_{min} is the minimum required time and t_p is the time proportionality of the mechanical stimulus $\gamma(\mathbf{x}, t)$.

To represent the maturation level of each cell during the time, t, the Maturation Index (MI) is defined as

$$\text{MI} = \begin{cases} \dfrac{t}{t_{\text{mat}}}, & t \leq t_{\text{mat}}, \\ 1, & t > t_{\text{mat}}. \end{cases} \tag{20}$$

The decision of the cellular phenotype adopted by the cell depends on the level of mechanical stimulus experienced by the cell during its maturation. For the different cellular phenotypes, their corresponding thresholds would be defined based on the mechanical characteristics of the tissue in which they live.[36] For example, osteoblasts, which basically reside within hard ECMs (30–45 kPa), only undergo low cell deformations.[3,4]

On the other hand, cellular apoptosis is the process by which the cell is able to trigger its own death in a controlled way.[58] This mechanism can be activated independently by each cell when detecting adverse situations for its integrity. For example, it has been observed that certain mechanical conditions cause the expression of proteins that trigger cellular apoptosis.[59] Likewise, it has been observed that the level of oxygen maintains a close relationship with cell survival, being able to trigger apoptosis under anoxia.[7,21,60] For this reason, the activation of apoptosis has been considered by both mechanical stimulation, through the mechanical signal, and by the chemical stimulus, through anoxia. Therefore, in this model, the cell will undergo apoptosis if $\gamma \geq \gamma_{\text{apop}}$ or $[o_2] \leq [o_2]_{\text{anox}}$, where γ_{apop} is the mechanical stimulus causing the cell death and $[o_2]_{\text{anox}}$ is the upper limit of the anoxia.

Based on experimental observations,[3,4,61] we assume that MSCs (m) are able to differentiate into osteoblasts (s) under certain mechanical and chemical conditions. Consequently, the process of MSC differentiation and apoptosis related to mechanical signals, oxygen concentration and MI can be represented by

$$\text{Cell state} = \begin{cases} s & \gamma_{\text{low}} < \gamma \leq \gamma_{\text{ost}} \text{ and } [o_2] \geq [o_2]_{\text{hyp}} \text{ and } \text{MI} = 1, \\ \text{No cell differentiation} & \text{Otherwise}, \end{cases} \tag{21}$$

where γ_{low} and γ_{ost} are the minimum and maximum mechanical stimulus for the differentiation of osteoblasts, while $[o_2]_{\text{hyp}}$ is the upper limit of hypoxia. It should be noted that small strains exerted cyclically on a typical cell might cause fatigue apoptosis[59] that we have not considered here.

The ECM is not only able to govern the processes of cellular differentiation but also plays a key role in the proliferation.[55] A cell is able to feel that it is in a favorable situation for growth and proliferation. For example, in a plate cell culture, cells proliferate until they reach coalescence, at such point, they stop proliferation.[62] As we commented before, the cells, through mechanotaxis, are able to recognize that they are surrounded by other cells, so that they stop the proliferation processes. In contrast, in the case of tumor cells, it has been observed that this mechanism fails, causing uncontrolled growth of the cells.[63,64] In an opposite situation, such as when cells are subjected to high strains, small cyclic strains or anoxia, cells are able to detect that they are in a harmful situation to their own integrity, triggering cellular apoptosis.[59,65]

When an injury occurs in a tissue, part of the cell population in the affected area dies and must be replaced by new cells during tissue regeneration. Cell proliferation is the mechanism by which cells are able to increase their population. An adult cell is able to duplicate its genetic content and, through the mitosis, divide itself to create two new cells. Thereby, the proliferation capacity of a cell depends on the degree of maturation of that cell. Although the mechanisms that regulate cell proliferation processes are still unclear, it has been observed that it depends on the mechanical stimuli experienced by the cell.[44,67,68] Thus, cell proliferation occurs when a certain threshold of mechanical stimuli is sensed by the cell. In the same way, it has been observed that the level of oxygen that the cell experiences plays a key role in this process, being able to increase or even inhibit cell proliferation.[7,14,21,27] Therefore, the cell proliferation related to mechanical stimulus, oxygen concentration and MI can be expressed by

$$\text{Cell proliferation} = \begin{cases} 1 \text{ mother cell } \rightarrow 2 \text{ daughter cells} & \gamma \leq \gamma_{\text{prol}} \text{ and } [o_2] \geq [o_2]_{\text{hyp}} \\ & \text{and MI} = 1 \\ \text{No cell division} & \text{Otherwise,} \end{cases} \tag{22}$$

where $i \in \{m, s\}$ and γ_i^{prol} is the mechanical stimulus that defines the proliferation limit of the ith cell.[31]

Once the proliferation is activated, the positions of the new two cells: $\mathbf{x}_{\text{daut}}^{(1)}$ and $\mathbf{x}_{\text{daut}}^{(2)}$, are defined as

$$\begin{aligned} \mathbf{x}_{\text{daut}}^{(1)} &= \mathbf{x}_{\text{moth}}, \\ \mathbf{x}_{\text{daut}}^{(2)} &= \mathbf{x}_{\text{moth}} + 2r\mathbf{e}_{\text{rand}}, \end{aligned} \tag{23}$$

where $\mathbf{x}_{\text{moth}}$ is the position of the mother cell and $\mathbf{e}_{\text{rand}}$ is a randomly defined unit vector.

3. Finite Element Implementation

For the implementation of the model, the commercial finite element software Abaqus[69] has been used through a user-defined element subroutine (UELM). The studied ECM, where the cells are included, has dimensions of $400 \times 200 \times 200\,\mu$m, meshed with a total of 16,000 regular hexahedral elements, with a total of 18,081 nodes. Each cell has been discretized from the ECM with 24 nodes on its surface (see Fig. 2(a)) and have constant spherical morphology. The calculation algorithm of this model is described in Fig. 4, and the properties used to calculate the mechanical behavior of the cells and the ECM are enumerated in Tables 1 and 2.

4. Numerical Examples

The purpose of the present model is to evaluate the effects of oxygen concentration on cell behavior. As observed, in experimental studies,[20,70,71] the oxygen concentration not only regulates the cell survival but also plays a key role in cell differentiation, proliferation and migration. For instance, osteoblasts under hypoxic conditions show a dramatic reduction in cell proliferation.[12] Using the present model, we will study the effects of the variation of oxygen concentration on cell

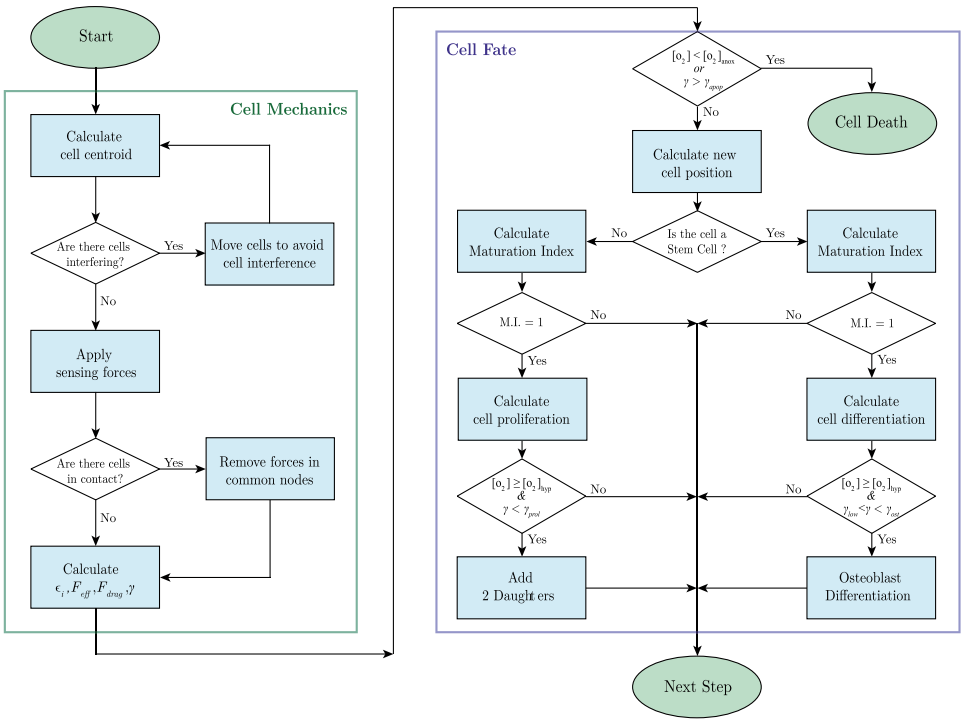

Fig. 4. The computational algorithm of the modeling of cell behavior divided into two parts: Cell mechanics and cell fate.

Table 1. Mechanical parameters of the model.

Parameter	Description	Value	Ref.
ν	ECM Poisson ratio	0.3	47, 48
η	ECM viscosity	1000 Pa·s	29, 48
K_{pas}	Stiffness of the passive elements of the cell	2.8 kPa	49
K_{act}	Stiffness of the actin–myosin machinery	2.0 kPa	49
$\varepsilon_{\max}$	Maximum strain of the cell	0.9	36, 50
$\varepsilon_{\min}$	Minimum strain of the cell	−0.9	36, 50
$\sigma_{\max}$	Maximum contractile stress exerted by the actin–myosin machinery	0.1 kPa	51, 52
$k_f = k_b$	Binding constant at the front and the rear of the cell	10^8 mol^{-1}	29
n_{r_f}	Number of available receptors at the front of the cell	1.5×10^5	29
n_{r_b}	Number of available receptors at the back of the cell	1.0×10^5	29
	Concentration of the ligands at the rear and the front of the cell	10^{-5} mol	29
$t_{\min}$	Minimum time needed for cell proliferation	4 days	31, 49
t_p	Time proportionality	200 days	31, 49

Table 2. Mechanical stimuli bounds that define the thresholds of the model.

Parameter	Description	Value	Ref.
γ_{low}	Lower bound of cell mechanical signal leading to osteoblast differentiation	0.005	31, 66
γ_{ost}	Upper bound of cell mechanical signal leading to osteoblast differentiation	0.04	31, 66
γ_{prol}	Maximum mechanical signal to cell proliferation	0.2	31
γ_{apop}	Cell mechanical signal leading to cell apoptosis	1.0	31
$[o_2]_{\text{hyp}}$	Upper limit of hypoxia	6.0%	12, 19
$[o_2]_{\text{anox}}$	Upper limit of anoxia	1.0%	19, 20

behavior to improve the current procedures of cell culture. For this aim, three numerical examples have been designed in which the effect of oxygen concentration, in a controlled environment, on cell behavior has been studied. In the first example, cell behavior is studied in a confined ECM without an oxygen supply. In this case, the cells consume the oxygen until it runs out (anoxia). In the second example, cell behavior is studied in a medium with a homogeneous and constant oxygen concentration (normoxia). Finally, in the third example, an oxygen gradient in the ECM is considered, simulating a bioreactor with oxygen supply located on one side of the ECM.

4.1. *Cell behavior within a confined ECM*

In the first numerical example, 10 MSCs have been randomly seeded in a confined ECM with a uniform stiffness of 45 kPa, which is suitable for the MSCs to be differentiated into osteoblast phenotype.[4,72] Each cell has the ability to migrate within the ECM due to a combination of mechanical and chemical stimuli.

Simultaneously, as explained above (see Fig. 4), they have the ability to differentiate, proliferate and die. To study the effect of different levels of oxygen concentration on cell behavior, a confined ECM in which the oxygen progressively decays during the assay, due to the cells' consumption, is considered. For this purpose, we have started with an initial oxygen concentration of 13%. In this case, the oxygen concentration falls progressively, passing through different levels of hypoxia until it reaches anoxia. During this process, the cell response, such as differentiation and proliferation, as well as apoptosis, are studied.

In the first phase of this example, cells were existing under normoxic conditions (6–13%[19,73]). While the cells are exposed to these concentrations, they show normal activity. For instance, MSCs received adequate mechanical (γ) and chemical ($[o_2]$) stimulus during the maturation inducing them to differentiate into osteoblasts[12,14] and then proliferate.[20,23] Therefore, as it is shown in Fig. 5(a), after five days of cells in culture, the cells started to differentiate into osteoblasts. During the successive days, all cells have been differentiated into osteoblasts effectively and subsequently began to proliferate. After 27 days, the concentration of oxygen falls below the limit of normoxia, leaving the cells exposed to hypoxic conditions. Under these conditions, the cells stop the proliferation process (see Figs. 5(b) and 8) maintaining the same number of cells. Due to the dramatic drop in oxygen concentration at the 40th day, most of the osteoblasts go through the process of apoptosis (see Fig. 5(c)).

4.2. *Cell behavior within an ECM with a uniform oxygen concentration (normoxia)*

The second numerical example has been designed to study the effect of long exposures to normoxic conditions on cell behavior. To this end, a constant oxygen concentration has been maintained throughout the experiment. This numerical example would be equivalent to the culture of the cells in a medium with controlled oxygen perfusion, which is the usual scheme in which the cells are maintained.[20,60,70] In this environment, we aim to carry out a more detailed study of the influence of normoxia on the processes of differentiation and proliferation of the cells. As mentioned before, MSCs have the ability to differentiate into different specialized cell types. The decision to differentiate into one cell type or the other, as well as the decision to not differentiate, is dictated by the capacity of the cell to recognize its environment. The cell can detect the rigidity of the ECM or the presence of external loads, as well as chemical cues, such as oxygen concentration or the presence of certain proteins in its environment. These stimuli can guide cell differentiation. In this case, we have applied the same mechanical conditions of the first case, but now we have considered constant normoxia oxygen concentration. As long as the concentration of oxygen stays above the limit of hypoxia ($[o_2]_{\text{hyp}}$), the cells will be able to differentiate and proliferate in the proper way.

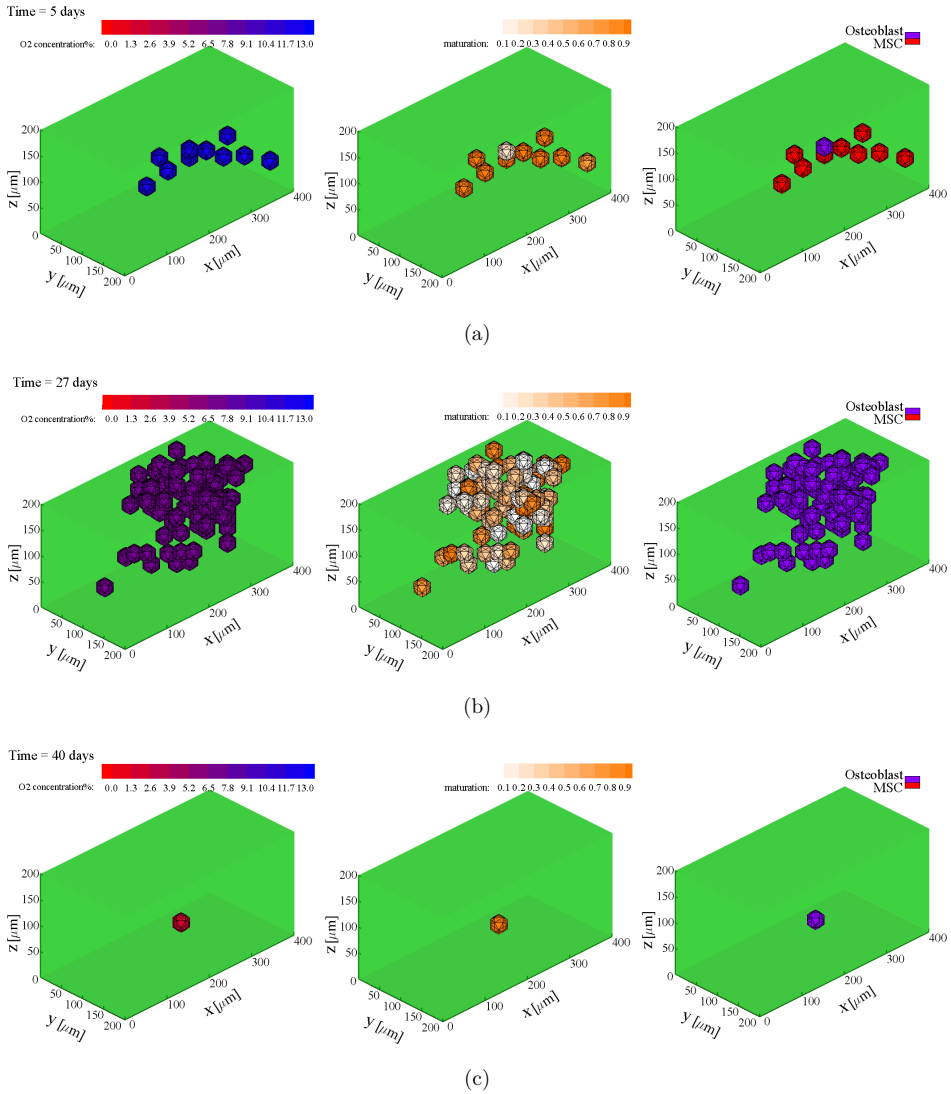

Fig. 5. Cell behavior within a confined ECM (see also video 1). Initially, 10 MSCs are randomly located within a confined ECM with a uniform stiffness of 45 kPa, free boundaries, and initial oxygen concentration of 13%. (a) After five days of cells in culture, the first MSC is maturated and differentiated into osteoblast as a response to its proper internal deformation (mechanical stimulus). (b) The MSCs continue the process of differentiation until all cells convert to osteoblast. Within the normoxia threshold, the osteoblast proliferates if the maturation is satisfied and the internal deformation is appropriate. (c) All osteoblasts go in the apoptosis process due to the catastrophic drop of oxygen concentration below anoxia threshold.

Therefore, as in the previous case, 10 cells were seeded randomly within an ECM with a stiffness of 45 kPa. In this example, a constant oxygen concentration of 21% has been considered during the experiment. In a similar way to the previous case, we can observe that some MSCs are differentiated into osteoblasts after five days (see

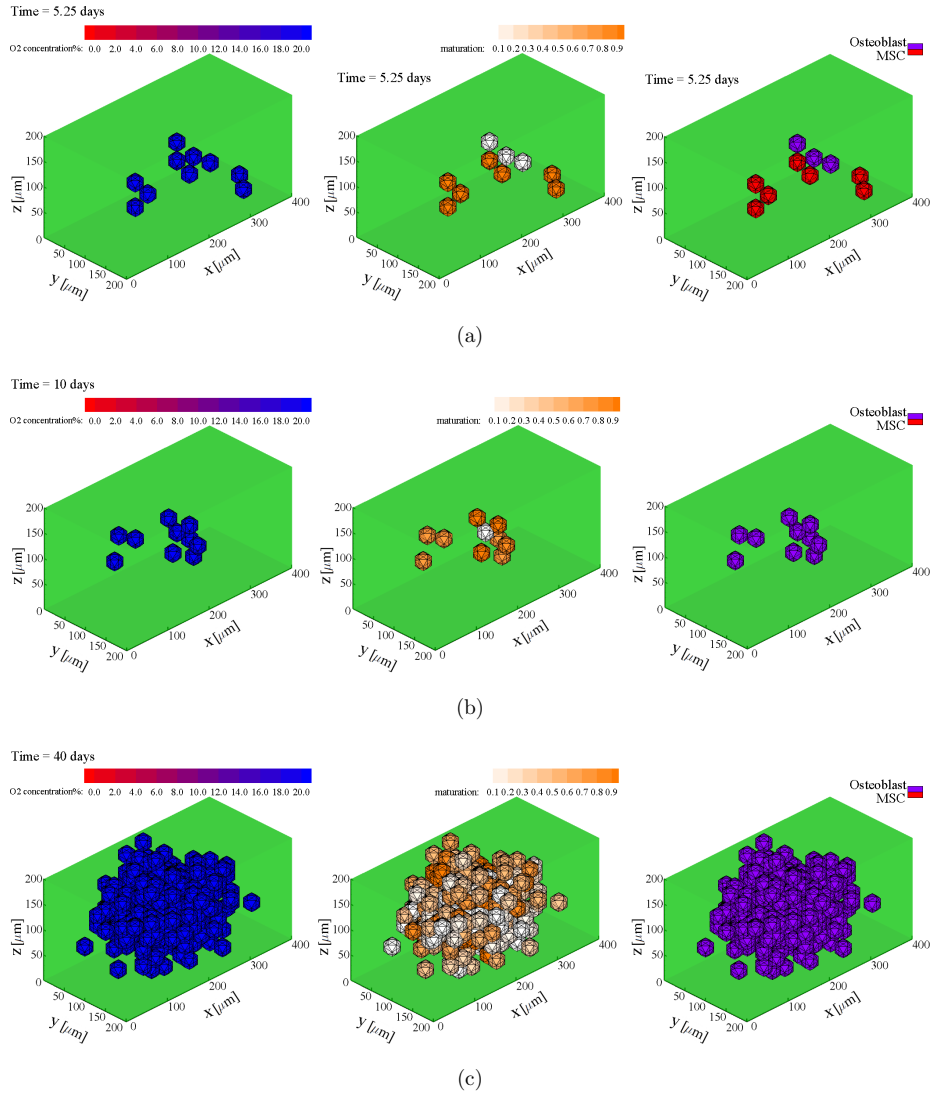

Fig. 6. Cell behavior within an ECM with a uniform oxygen concentration (normoxia) (see also video 2). In the beginning, 10 MSCs randomly reside within an ECM with a uniform stiffness of 45 kPa and free boundaries. It is assumed that there is a uniform oxygen concentration of 21% within the ECM. (a) After five days, several MSCs differentiate into osteoblast as a response to the appropriate internal deformation and the maturation. (b) MSCs continue the differentiation process and each osteoblast proliferates if the maturation is satisfied and the internal deformation is appropriate since the oxygen concentration does not drop below the normoxia threshold. (c) Osteoblasts concentration after 40 days.

Fig. 6(a)). In the consecutive days, once the cells reach the appropriate level of maturity, they continue to differentiate. On day 10, it can be seen how all the cells have differentiated (see Fig. 6(b)). Subsequently, the cells begin to proliferate until the end of the experiment. Because there is no decrement in the oxygen level,

proliferation is only limited by the mechanical conditions of the environment. Finally, on day 40, it is observed that there is a great concentration of cells in the center of the ECM where they sense less internal deformation (see Figs. 6(c) and 8).

4.3. *Cell behavior within an ECM with oxygen gradient (from anoxia to normoxia)*

In the third case, different levels of oxygen concentration have been considered creating a gradient of oxygen concentrations in x-direction, which changes from anoxia to normoxia. In this scenario, the cells tend to migrate to zones of higher oxygen concentration to ensure their viability. Within this profile of oxygen concentration, anoxia, hypoxia and normoxia conditions will occur at the same time but in different zones of the ECM. In this way, it is possible to study cell behavior in these three regimens depending on the location of the cell. Cells in the area under conditions of anoxia will trigger apoptosis while cells on the opposite side of the ECM, where they are under normoxic conditions, will differentiate and proliferate properly. Between the two extremes, under conditions of hypoxia, the cells will tend to migrate toward higher oxygen concentration, activating differen-tiation and proliferation when they cross the threshold of hypoxia. Volkmer *et al.*,[73] performing a static analysis on a bioreactor, observed these cell behaviors by sub-jecting the culture to a gradient of oxygen concentrations between 0% and 21%. They observed that in zones under conditions of anoxia, the cells triggered apoptosis while in the area with high concentrations of oxygen the cells are accumulated.

As in the previous cases, 10 MSCs have been randomly seeded within an ECM with a stiffness of 45 kPa. An oxygen concentration of 0% has been considered in the plane at $x = 0$ (X_0) while a concentration of 21% has been considered in the opposite plane at $x = 400\,\mu$m (X_{400}), establishing a linear gradient of oxygen concentration along the x-direction. At the beginning of the simulation, the cells that are close to the X_0 plane could trigger apoptosis due to the low oxygen concentration, depending on its initial position. During the simulation, one of the cells migrates toward the X_0 plane, due to the effects of the protrusion force, causing cell apoptosis (see Figs. 7(a) and 8). Generally, the cells tend to migrate toward the X_{400} plane, due to the effect of chemotaxis, where the concentration of oxygen is maximum. This is consistent with the experimental results.[73–75] On day 5, most of the cells are in the normoxia zone after having migrated from their initial position (see Fig. 7(b)). As in the previous cases, after five days, the cells begin to differentiate into osteoblasts. During the following days, the cells end up differentiating themselves as they reach zones of normoxic conditions. Once all the cells are near to the X_{400} plane, the cells migrate close to the plane without moving away. The proliferation of cells near the plane causes a high concentration of cells in this part of the ECM, while the rest of the ECM remains empty (see Fig. 7(c)). At the end of the 40 days of the experiment, the cells reach the highest population (see Fig. 8) in the

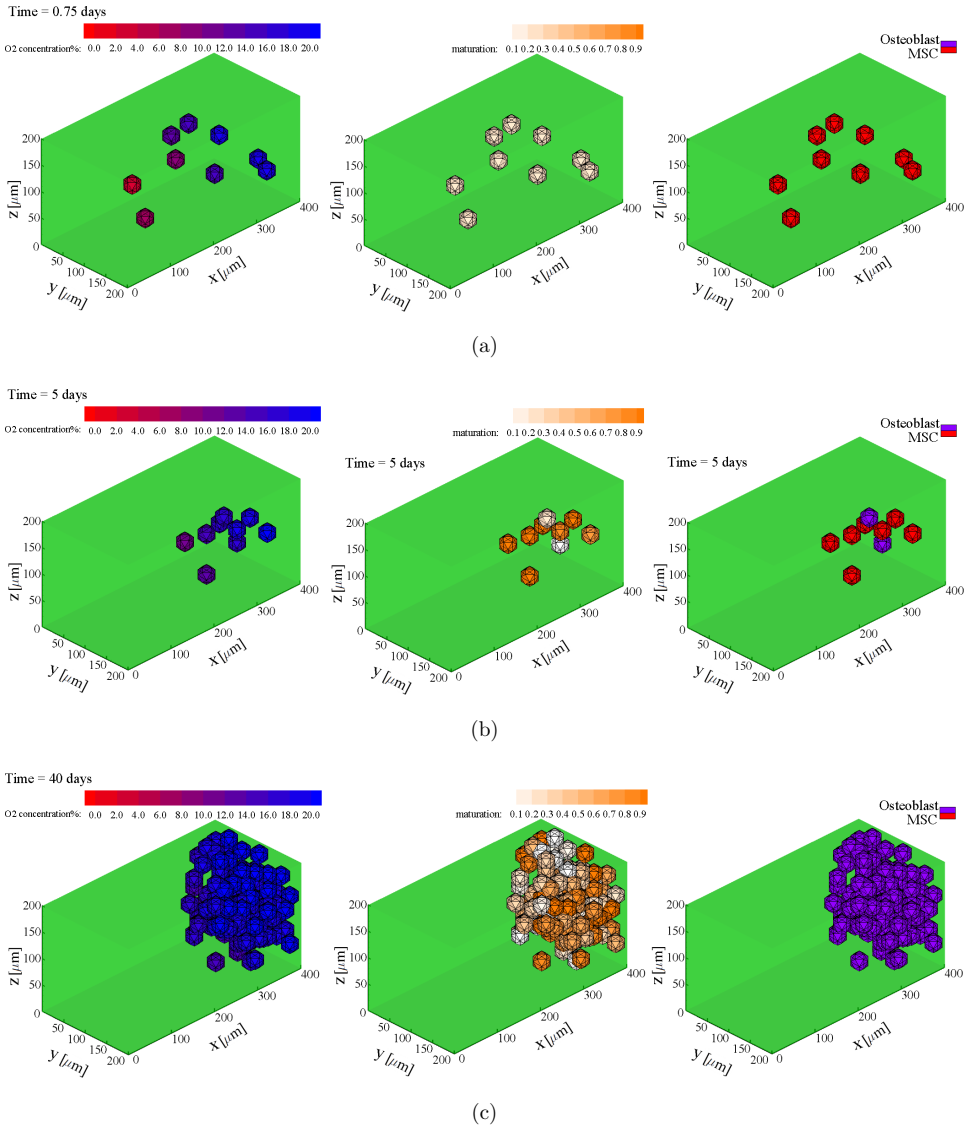

Fig. 7. Cell behavior within an ECM with oxygen gradient (from anoxia to normoxia) (see also video 3). Initially, 10 MSCs randomly reside within an ECM with a uniform stiffness of 45 kPa and free boundaries. It is assumed that at $x = 0$ oxygen concentration is zero while the surface at $x = 400\,\mu$m is subjected to an oxygen source of 21%. This difference produces an oxygen gradient in the direction of the x-axis. Oxygen gradient actively directs MSCs toward the maximum oxygen concentration at $x = 400\,\mu$m. The protrusion force randomly directs one MSC toward the surface with minimum oxygen concentration causing its death on the first day (a). MSCs directionally migrate to higher oxygen concentration. Once the cell reaches the region with normoxia, if the cell is maturated enough, they differentiate into osteoblasts (b). Finally, osteoblasts tend to keep the position as close as the surface with maximum oxygen concentration and proliferate (c).

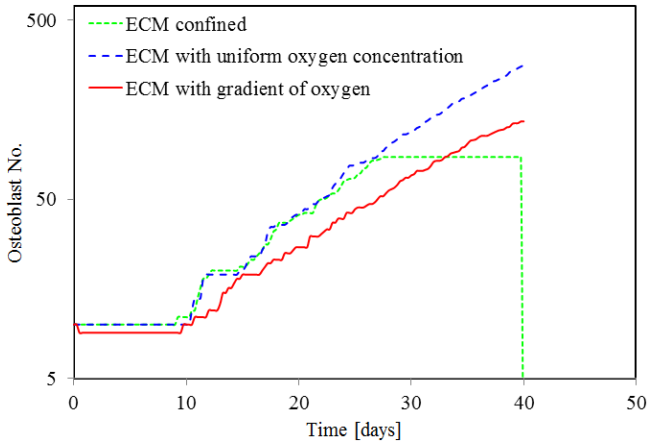

Fig. 8. Cell number versus time within an ECM with a uniform stiffness of 45 kPa and with a different control of the oxygen concentration. The results show that, in the confined ECM, the cell has the lowest rate of cell proliferation while they have the highest proliferation rate within an ECM with uniform oxygen concentration. (see also videos 1, 2 and 3).

zone with normoxia conditions, keeping close to the plane of the maximum concentration of oxygen all the time. Because this plan is unconstrained, osteoblast senses higher internal deformation, which in turn decreases the proliferation rate.

5. Conclusions

Oxygen is an essential element for cell development. Several studies have revealed that oxygen plays a key role in tissue regeneration. Different thresholds of oxygen concentration effectively influence cell survival and viability.[60,73] Besides, it has also been shown that oxygen concentration has an important influence on the differentiation of MSC, being a key factor in the identification of tissues. Thereby, MSC differentiation and proliferation, as well as osteoblast proliferation and migration, can be guided through their stimulation through different thresholds of oxygen concentration.[14,76] Therefore, oxygen should be considered as a key stimulus in the regulation of the processes of differentiation, proliferation, migration and apoptosis.

In this work, a 3D computational model has been developed and employed to study the cell response to the alterations of the oxygen concentration during cell culture. The model takes into account the different biological processes of the cell in culture, such as cell migration, interaction, differentiation, proliferation and apoptosis. In the presented model, the mechanical and chemical stimuli that the cell experiences are included simultaneously. Using this model, we can get closer to the understanding of the effect of the ECM properties on cell behavior. The obtained results are qualitatively in line with the experimental studies.[4,19,20,60,71,73,77] The model has been shown to be able to give consistent results under different oxygen

conditions. Here, we should emphasize that by means of numerical simulations, we can improve the experimental results, saving time and costs. Besides, we can achieve a better understanding of cellular behavior, the role played by the ECM and the stimuli that the cell receives from its surrounding. Such models can be an effective tool for interpreting, corroborating and providing new insights and conclusions of great utility for cellular research. For this purpose, three numerical experiments have been designed and developed. Many interesting results and conclusions have been obtained. As expected, it has been observed that cells within a confined ECM show low cell proliferation, while the cells in the ECM with homogeneous normoxia conditions show the highest cellular proliferation. Besides, it has observed that, while normoxia conditions are maintained in the ECM, the cell number within confined and homogeneous ECM are mostly similar (see Fig. 8). These two cases also present the same tendency of cellular migration, where the cells tend to migrate to the center of the ECM forming an accumulation. In the absence of a chemical gradient, the cells respond mainly to the rigidity of the ECM through mechanotaxis. Therefore, they migrate toward the center of the ECM, where they feel more fixed and undergo less internal deformation than near to the free boundaries. Comparing the migration tendencies of the second and third cases, it can be con-cluded that the effects of chemotaxis, produced by the oxygen gradient, have greater weight in the migration of the cells. It has been noted that the cells tend to migrate toward the plane with the highest oxygen concentration and remain close to it. As this plane is an unconstrained plane, nearby cells undergo a greater internal deformation, which results in slower maturation of the cells and consequently decreases the cell proliferation. It should also be noted that the direction of cells migration is not completely controlled by chemotaxis, but they also present an irregular migratory behavior. This irregular behavior in migration is due to the combination of protrusion forces and cell–cell interaction. Both effects of hypoxia and anoxia have been shown in the case of the confined ECM and in the case of the gradient of oxygen concentration. Thus, under hypoxic conditions, we observed inhibition of cell proliferation and differentiation. As observed in the last example, under anoxic conditions, the cells trigger apoptosis.

Taken together, the results of the model presented here and the earlier experimental observations show that oxygen concentration plays a significant role in controlling cell behavior. Accordingly, the present 3D numerical model can successfully predict essential aspects of cell migration, interaction, maturation, differentiation, proliferation and apoptosis during regenerative events. We believe that the present model provides one-step forward in computational methodology to simultaneously consider the different features of cell behavior in the presence of mechanotactic and chemotactic cues. Although more sophisticated experimental studies are required to calibrate this model quantitatively, general aspects of the results discussed here are qualitatively consistent with documented experimental findings.

Acknowledgments

The authors gratefully acknowledge the financial support from the Spanish Ministry of Economy and Competitiveness (MINECO MAT2016-76039-C4-4-R, AEI/FEDER, UE), the Government of Aragon (DGA-T24_17R) and the Biomedical Research Networking Center in Bioengineering, Biomaterials and Nanomedicine (CIBER-BBN). CIBER-BBN is financed by the Instituto de Salud Carlos III with assistance from the European Regional Development Fund.

References

1. Salisbury Palomares KT, Gleason RE, Mason ZD, Cullinane DM, Einhorn TA, Gerstenfeld LC, Morgan EF, Mechanical stimulation alters tissue differentiation and molecular expression during bone healing, *J Orthop Res* **27**(9):1123–1132, 2009.
2. Li D, Zhou J, Chowdhury F, Cheng J, Wang N, Wang F, Role of mechanical factors in fate decisions of stem cells, *Regen Med* **6**:229–240, 2011.
3. Huebsch N, Arany PR, Mao AS, Shvartsman D, Ali OA, Bencherif SA, Rivera-Feliciano J, Mooney DJ, Harnessing traction-mediated manipulation of the cell/matrix interface to control stem-cell fate, *Nat Mater* **9**:518–526, 2010.
4. Engler AJ, Sen S, Sweeney HL, Discher DE, Matrix elasticity directs stem cell lineage specification, *Cell* **126**:677–689, 2006.
5. Pittenger MF, Mackay AM, Beck SC, Jaiswal RK, Douglas R, Mosca JD, Moorman MA, Simonetti DW, Craig S, Marshak DR, Multilineage potential of adult human mesenchymal stem cells, *Science* **284**(5411):143–147, 1999.
6. Pierce JH, Di Marco E, Cox GW, Lombardi D, Ruggiero M, Varesio L, Wang LM, Choudhury GG, Sakaguchi AY, Di Fiore PP, Aaronson SA, Macrophage-colony-stimulating factor (CSF-1) induces proliferation, chemotaxis, and reversible monocytic differentiation in myeloid progenitor cells transfected with the human c-fms/CSF-1 receptor cDNA, *Proc Natl Acad Sci USA* **87**:5613–5617, 1990.
7. Ray JB, Arab S, Deng Y, Liu P, Penn L, Courtman DW, Ward ME, Oxygen regulation of arterial smooth muscle cell proliferation and survival, Am J Physiol Heart Circ Physiol 294: H839–H852, 2008.
8. Hubbi ME, Semenza GL, Regulation of cell proliferation by hypoxia-inducible factors, *Am J Physiol Cell Physiol* **309**(12):C775–C782, 2015.
9. Higazi AA, Kniss D, Manuppello J, Barnathan ES, Cines DB, Thermotaxis of human trophoblastic cells, *Placenta* **17**(8):683–687, 1996.
10. Zhao M, Electrical fields in wound healing — An overriding signal that directs cell migration, Semin Cell Dev Biol 20(6):674-82, 2009.
11. Stoppel WL, Kaplan DL, Black LD, Electrical and mechanical stimulation of cardiac cells and tissue constructs, *Adv Drug Deliv Rev* **96**:135–155, 2016.
12. Utting JC, Robins SP, Brandao-Burch A, Orriss IR, Behar J, Arnett TR, Hypoxia inhibits the growth, differentiation and bone-forming capacity of rat osteoblasts, *Exp Cell Res* **312**(10):1693–1702, 2006.
13. Wan C, Gilbert SR, Wang Y, Cao X, Shen X, Ramaswamy G, Jacobsen KA, Alaql ZS, Eberhardt AW, Gerstenfeld LC, Einhorn TA, Deng L, Clemens TL, Activation of the hypoxia-inducible factor — 1alpha pathway accelerates bone regeneration, *Proc Natl Acad Sci USA* **105**(2):686–691, 2008.
14. Malda J, Klein TJ, Upton Z, The roles of hypoxia in the *in vitro* engineering of tissues, *Tissue Eng* **13**(9):2153–2162, 2007.

15. Carter DR, Blenman PR, Beaupré GS, Correlations between mechanical stress history and tissue differentiation in initial fracure healing, *J Ortho Res* **6**(5):736–748, 1988.
16. Kelly D, Prendergast P, Mechano-regulation of stem cell differentiation and tissue regeneration in osteochondral defects, *J Biomech* **38**:1413–1422, 2005.
17. Maul TM, Chew DW, Nieponice A, Vorp DA, Mechanical stimuli differentially control stem cell behavior: Morphology, proliferation, and differentiation, *Biomech Model Mechanobiol* **10**:939–953, 2011.
18. Raeber GP, Lutolf MP, Hubbell JA, Molecularly engineered PEG hydrogels: A novel model system for proteolytically mediated cell migration, *Biophys J* **89**(2):1374–1388, 2005.
19. Lee CM, Genetos DC, You Z, Yellowley CE, Hypoxia regulates PGE2 release and EP1 receptor expression in osteoblastic cells, *J Cell Phys* **212**:182–188, 2007.
20. Salim A, Nacamuli RP, Morgan EF, Giaccia AJ, Longaker MT, Transient changes in oxygen tension inhibit osteogenic differentiation and Runx2 expression in osteoblasts, *J Biol Chem* **279**:40007–40016, 2004.
21. Schmaltz C, Hardenbergh PH, Wells A, Fisher DE, Regulation of proliferation-survival decisions during tumor cell hypoxia, *Mol Cell Biol* **18**(5):2845–2854, 1998.
22. Sun Y, Wang H, Liu M, Lin F, Hua J, Resveratrol abrogates the effects of hypoxia on cell proliferation, invasion and EMT in osteosarcoma cellsthrough downregulation of the HIF-1α protein, *Mol Med Rep* **11**(3):1975–1981, 2015.
23. Steinbrech DS, Mehrara BJ, Saadeh PB, Chin G, Dudziak ME, Gerrets RP, Gittes GK, Longaker MT, Hypoxia regulates VEGF expression and cellular proliferation by osteoblasts *in vitro*, *Plastic Reconstruct Surg* **104**(3):738–747, 1999.
24. Bradley TR, Hodgson GS, Rosendaal M, The effect of oxygen tension on haemopoietic and fibroblast cell proliferation *in vitro*, *J Cell Physiol* **97**(3) Pt 2 Suppl 1:517–522, 1978.
25. Bosgraaf L, van Haastert PJ, Navigation of chemotactic cells by parallel signaling to pseudopod persistence and orientation, *PLoS ONE* **4**:e6842, 2009.
26. Neilson MP, Veltman DM, van Haastert PJ, Webb SD, Mackenzie JA, Insall RH, Chemotaxis: A feedback-based computational model robustly predicts multiple aspects of real cell behaviour, *PLoS Biol* **9**:e1000618, 2011.
27. Warren SM, Steinbrech DS, Mehrara BJ, Saadeh PB, Greenwald JA, Spector JA, Bouletreau PJ, Longaker MT, Hypoxia regulates osteoblast gene expression, *J Surg Res* **99**(1):147–155, 2001.
28. Galbusera F, Cioffi M, Raimondi MT, An in silico bioreactor for simulating laboratory experiments in tissue engineering, *Biomed Microdev* **10**:547–554, 2008.
29. Zaman MH, Kamm RD, Matsudaira P, Lauffenburger DA, Computational model for cell migration in three-dimensional matrices, *Biophys J* **89**(2):1389–1397, 2005.
30. Mousavi SJ, Doweidar MH, Doblaré M, Computational modelliComput Methods Biomech Biomed Engin, 17(6):678-93, 2014nd analysis of me-chanical conditions on cell locomotion and cell–cell interaction, 2014.
31. Kang KT, Park JH, Kim HJ, Lee HM, Lee KI, Jung HH, Lee HY, Jang JW, Study of tissue differentiation of mesenchymal stem cells by mechanical stimuli and an algorithm for bone fracture healing, *Tissue Eng Regen Med* **8**(4):359–370, 2011.
32. Ali N, Zaman A, Sajid M, Bég OA, Shamshuddin M, Kadir A, numerical simulation of time-dependent non-newtonian nanopharmacodynamic transport phenomena in a tapered overlapping stenosed artery, *Nanosci Technol Int J* **9**(3):247–282, 2018.
33. Sheikholeslami M, Rokni HB, CVFEM for effect of Lorentz forces on nanofluid flow in a porous complex shaped enclosure by means of non-equilibrium model, *J Mol Liquids* **254**:446–462, 2018.
34. Mousavi SJ, Doweidar MH, Doblaré M, 3D computational modelling of cell migration: A mechano-chemo-thermo-electrotaxis approach, *J Theor Biol* **329**:64–73, 2013.

35. Mousavi SJ, Doblaré M, Hamdy Doweidar M, Computational modelling of multi-cell migration in a multi-signalling substrate, *Phys Biol* **11**(2):026002, 2014.
36. Mousavi SJ, Hamdy Doweidar M, Role of mechanical cues in cell differentiation and proliferation: A 3D numerical model, *PLoS ONE* **10**:e0124529, 2015.
37. Mousavi SJ, Doweidar MH, Doblaré M, Cell migration and cell-cell interaction in the presence of mechano-chemo-thermotaxis., *Mol Cell Biomech* **10**:1–25, 2013.
38. Mousavi SJ, Doweidar MH, A novel mechanotactic 3D modeling of cell morphology, *Phys Biol* **11**:046005, 2014.
39. Mousavi SJ, Doweidar MH, Three-dimensional numerical model of cell morphology during migration in multi-signaling substrates, *PLoS ONE* **10**:e0122094, 2015.
40. Bernheim-Groswasser A, Prost J, Sykes C, Mechanism of actin-based motility: A dynamic state diagram, *Biophys J* **89**(2):1411–1419, 2005.
41. Mogilner A, Mathematics of cell motility: Have we got its number? *J Math Biol* **58**(1–2):105–134, 2009.
42. Gao RC, Zhang XD, Sun YH, Kamimura Y, Mogilner A, Devreotes PN, Zhao M, Different roles of membrane potentials in electrotaxis and chemotaxis of Dictyostelium cells, *Eukaryotic Cell* **10**(9):1251–1256, 2011.
43. Gumbiner BM, Cell adhesion: The molecular basis of tissue architecture and morphogenesis, *Cell* **84**:345–357, 1996.
44. Geiger B, Bershadsky A, Exploring the neighborhood: Adhesion-coupled cell mechanosensors, Cell, 110(2):139-42, 2002.
45. Mogilner A, Rubinstein B, The physics of filopodial protrusion, *Biophys J* **89**(2):782–795, 2005.
46. DiMilla PA, Barbee K, Lauffenburger DA, Mathematical-model for the effects of adhesion and mechanics on cell-migration speed, *Biophys J* **60**(1):15–37, 1991.
47. Akiyama SK, Yamada KM, The interaction of plasma fibronectin with fibroblastic cells in suspension, *J Biolog Chem* **260**(7):4492–4500, 1985.
48. Ulrich TA, De Juan Pardo EM, Kumar S, The mechanical rigidity of the extracellular matrix regulates the structure, motility, and proliferation of glioma cells, *Cancer Res* **69**(10):4167–4174, 2009.
49. Schäfer A, Radmacher M, Influence of myosin II activity on stiffness of fibroblast cells, *Acta Biomater* **1**(3):273–280, 2005.
50. Ramtani S, Mechanical modelling of cell/ECM and cell/cell interactions during the contraction of a fibroblast-populated collagen microsphere: Theory and model simulation, *J Biomech* **37**(11):1709–1718, 2004.
51. Oster GF, Murray JD, Harris AK, Mechanical aspects of mesenchymal morphogenesis, *J Embryol Exp Morphol* **78**(1):83–125, 1983.
52. Georges PC, Janmey PA, Cell type-specific response to growth on soft materials, *J Appl Physiol* **98**(4):1547–1553, 2005.
53. Brodland GW, Wiebe CJ, Mechanical effects of cell anisotropy on epithelia, *Comput Methods Biomech Biomed Eng* **7**(2):91–99, 2004.
54. Palsson E, A three-dimensional model of cell movement in multicellular systems, *Future Gen Comput Syst* **17**:835–852, 2001.
55. Delaine-Smith RM, Reilly GC, Mesenchymal stem cell responses to mechanical stimuli, *Muscles Ligaments Tendons J* **2**:169–80, 2012.
56. Claes LE, Heigele CA, Magnitudes of local stress and strain along bony surfaces predict the course and type of fracture healing, *J Biomech* **32**(3):255–266, 1999.
57. Wu QQ, Chen Q, Mechanoregulation of chondrocyte proliferation, maturation, and hypertrophy: Ion-channel dependent transduction of matrix deformation signals, *Exp Cell Res* **256**:383–391, 2000.

58. Elmore S, Apoptosis: A review of programmed cell death, Toxicol Pathol, 35(4):495-516, 2007.
59. Kearney EM, Prendergast PJ, Campbell VA, Mechanisms of strain-mediated mesenchymal stem cell apoptosis, *J Biomech Eng* **130**(6):061004, 2008.
60. Zhu W, Chen J, Cong X, Hu S, Chen X, Hypoxia and Serum Deprivation-Induced Apoptosis in Mesenchymal Stem Cells, *Stem Cells* **24**:416–425, 2006.
61. Lee DA, Knight MM, Campbell JJ, Bader DL, Stem cell mechanobiology, *J Cell Biochem* **112**(1):1–9, 2011.
62. Aragona M, Panciera T, Manfrin A, Giulitti S, Michielin F, Elvassore N, Dupont S, Piccolo S, A mechanical checkpoint controls multicellular growth through YAP/TAZ regulation by actin-processing factors, *Cell* **154**:1047–1059, 2013.
63. Low BC, Pan CQ, Shivashankar GV, Bershadsky A, Sudol M, Sheetz M, YAP/TAZ as mechanosensors and mechanotransducers in regulating organ size and tumor growth, *FEBS Lett* **588**(16):2663–2670, 2014.
64. Abercrombie M, Contact inhibition and malignancy, *Nature* **281**(5729):259–262, 1979.
65. Gladman SJ, Ward RE, Michael-Titus AT, Knight MM, Priestley JV, The effect of mechanical strain or hypoxia on cell death in subpopulations of rat dorsal root ganglion neurons in vitro, *Neuroscience* **171**:577–587, 2010.
66. Isaksson H, Wilson W, van Donkelaar CC, Huiskes R, Ito K, Comparison of biophysical stimuli for mechano-regulation of tissue differentiation during fracture healing, *J Biomech* **39**(8):1507–1516, 2006.
67. Puetzer JL, Petitte JN, Loboa EG, Comparative review of growth factors for induction of three-dimensional *in vitro* chondrogenesis in human mesenchymal stem cells isolated from bone marrow and adipose tissue, *Tissue Eng B Rev* **16**:435–444, 2010.
68. Chen CS, Tan J, Tien J, Mechanotransduction at cell-matrix and cell–cell contacts, *Annu Rev Biomed Eng* **6**(1):275–302, 2004.
69. DS SIMULIA Corp, *Abaqus 6.11. Theory Manual*, 2011.
70. Agudo-López A, Miguel BG, Fernández I, Martínez AM, Role of protein kinase C and mitochondrial permeability transition pore in the neuroprotective effect of ceramide in ischemia-induced cell death, *FEBS Lett* **585**:99–103, 2011.
71. Jonitz A, Lochner K, Lindner T, Hansmann D, Marrot A, Bader R, Oxygen consumption, acidification and migration capacity of human primary osteoblasts within a three-dimensional tantalum scaffold, *J Mater Sci Mater Med* **22**:2089–2095, 2011.
72. Buxboim A, Ivanovska IL, Discher DE, Matrix elasticity, cytoskeletal forces and physics of the nucleus: How deeply do cells 'feel' outside and in? *J Cell Sci* **123**(3):297–308, 2010.
73. Volkmer E, Drosse I, Otto S, Stangelmayer A, Stengele M, Kallukalam BC, Mutschler W, Schieker M, Hypoxia in static and dynamic 3D culture systems for tissue engineering of bone, *Tissue Eng A* **14**(8):1331–1340, 2008.
74. Oppegard SC, Eddington DT, A microfabricated platform for establishing oxygen gradients in 3-D constructs, *Biomed Microdev* **15**:407–414, 2013.
75. Ayuso JM, Monge R, Martínez-González A, Virumbrales-Muñoz M, Llamazares GA, Berganzo J, Hernández-Laín A, Santolaria J, Doblaré M, Hubert C, Rich JN, Sánchez-Gómez P, Pérez-García VM, Ochoa I, Fernández LJ, Glioblastoma on a microfluidic chip: Generating pseudopalisades and enhancing aggressiveness through blood vessel obstruction events, *Neuro-Oncology* **19**(4):503–513, 2017.
76. Bassett C, Herrmann I, Influence of oxygen concentration and mechanical factors on differentiation of connective tissues *in vitro*, *Nature* **190**:460–461, 1961.
77. Schirrmacher K, Lauterbach S, Bingmann D, Oxygen consumption of calvarial bone cells *in vitro*, *J Orthop Res* **15**:558–562, 1997.